Published in final edited form as:
Atherosclerosis. 2009 November ; 207(1): 139–143. doi:10.1016/j.atherosclerosis.2009.04.023.

Multimodality imaging of atherosclerotic plaque activity and composition using FDG-PET/CT and MRI in carotid and femoral arteries

Stephane S. Silvera, MD[*], **Hamza el Aidi, BS**[*], **James H. F. Rudd, MD, PhD**[*], **Venkatesh Mani, PhD**[*], **Lingde Yang, MD**[*], **Michael Farkouh, MD, MSC**[†], **Valentin Fuster, MD, PHD**[§], and **Zahi A. Fayad, PHD, FACC, FAHA**[*]

[*]Imaging Science Laboratories, Mount Sinai School of Medicine, New York, New York

[†]Cardiovascular Imaging Clinical Trials Unit, Mount Sinai School of Medicine, New York, New York

[§]The Zena and Michael A. Wiener Cardiovascular Institute and Marie-Josee and Henry R. Kravis Cardiovascular Health Center, Mount Sinai School of Medicine, New York, New York

Abstract

Purpose—To evaluate the relationship between atherosclerotic plaque inflammation, as assessed by FDG-Positron Emission Tomography/Computed Tomography (FDG-PET/CT), and plaque morphology and composition, as assessed by magnetic resonance imaging (MRI), in the carotid and femoral arteries.

Materials and methods—Sixteen patients underwent FDG-PET/CT and MRI (T2 weighted (T2W) and Proton density weighted (PDW)) of the carotid and femoral arteries. For every image slice, two observers determined the corresponding regions of the FDG-PET/CT and MRI image sets by matching CT and T2W axial images. Each plaque was then classified into one of three groups according to the CT appearance and T2W/PDW signal: 1) collagen, 2) lipid-necrotic core and 3) calcium.

Arterial FDG uptake was measured for each plaque and normalized to vein FDG activity to produce a blood-normalized artery activity called the target to background ratio (TBR). The vessel wall thickness (VWT), the vessel wall area and the total vessel wall area were measured from the T2W MR images.

Results—The TBR value was higher in the lipid-necrotic core group compared to the collagen and calcium groups, ($p < 0.001$). The lipid-necrotic core group demonstrated a significant TBR variation according to the median of the VWT (TBR = 1.26 ± 0.25 vs. TBR = 1.50 ± 0.12). There was no correlation with other morphological MR parameters.

Conclusions—This study demonstrates the complementary value of non-invasive FDG-PET/CT and MR imaging for the evaluation of atherosclerotic plaque composition and activity. Lipid-rich plaques are more inflamed than either calcified or collagen-rich plaques.

Corresponding author info: Zahi A. Fayad, PHD, FACC, FAHA, Fax: 212 534 2683 Tel: 212 241 7717, Zahi.Fayad@mssm.edu. **Institution:** Sinai Translational and Molecular Imaging Institute and Imaging Science Laboratories, Mount Sinai School of Medicine, One Gustave L. Levy Place, New York, New York 10029, USA

Introduction

Atherosclerosis remains the commonest cause of death in the western world[1, 2]. It has origins in childhood but usually remains asymptomatic until it has reached an advanced pathological stage. Whilst early intervention can reduce mortality and morbidity[3, 4], the lack of symptoms early in the disease course makes it difficult to target all affected patients. Inflamed plaques, and those with large lipid cores and thin fibrous caps are more likely to progress and cause clinical events than those without these features[5–8]. Therefore imaging the vasculature for both its inflammatory state (activity) and the presence of disease is becoming more important[9].

Positron Emission Tomography/ Computed Tomography imaging (PET/CT) can identify and track inflammation within atherosclerotic plaque when used with the tracer [^{18}F]-Fluoro-2-deoxy-D-glucose (FDG). This radionuclide is able to accumulate within metabolically active cells, including plaque macrophages. Rudd et al. demonstrated enhanced carotid FDG uptake in patients with recent ischemic cerebrovascular events[10]. Subsequent studies have shown a good agreement between FDG uptake and plaque macrophage content in a similar patient group ($r = 0.78$, $p<0.001$)[11].

Magnetic Resonance Imaging (MRI) can identify high-risk atherosclerotic plaques. Yuan et al. showed in an in-vivo multicontrast magnetic resonance study of human carotid arteries a sensitivity of 85% and a specificity of 92% for identifying plaques with high risk features such as a lipid-necrotic core [12]. Similarly, Cai et al. demonstrated good agreement between the American Heart Association (AHA) classifications of plaques and parameters derived from MRI [13]. We set out to examine the relationship between inflammation, plaque morphology and composition using FDG-PET/CT and MRI of the carotid and femoral arteries. We hypothesized that highly inflamed plaques on PET would have the largest lipid rich areas on MRI.

Methods

Study population

We recruited 16 patients (11 men, 5 women; mean age, 63.1 years (SD±9.6 years)) with cardiovascular risk factors (Table 1). All patients had PET/CT and MR studies performed the same day. Informed consent was obtained and the study was approved by the local Institutional Review Board. Femoral imaging was performed if femoral atherosclerotic disease was clinically documented (7 subjects). Carotid imaging was performed in the remaining nine patients without femoral artery disease. Those remaining patients were referred because of a recent history of myocardial infarction (<3 months).

PET/CT imaging

PET/CT was performed after an overnight fast using a General Electric (Milwaukee, Wisconsin) Lightspeed discovery ST[16] PET/CT scanner. The serum glucose was measured before FDG administration; patients with a level of ≥200 mg/dl were excluded. FDG was administered intravenously (12.8 to 18 mCi), and patients rested comfortably for 90 min. The circulation time was based on previous studies as giving an optimal signal to background FDG uptake ratio [15]. A CT scan (140Kv, 80mA, and 4.25mm slice thickness) was performed for attenuation correction and coregistration. Femoral imaging covered the area from the aortic bifurcation to the knee, in 2D mode over 40 minutes acquisition time. Carotid imaging covered one bed position (15.5cm) with the superior aspect being the internal auditory meatus and was acquired in 3D mode using a 128 × 128 pixel matrix. 3D PET images were reconstructed using the backprojection algorithm[16] while 2D PET images

were reconstructed using the ordered subset–expectation maximization (OS-EM) algorithm[17].

MRI imaging

MR was performed on a 1.5 Tesla Siemens Sonata MR system (Siemens, Erlangen, Germany; maximum gradient amplitude = 40 mT/m; slew rate = 200 mT/m/ms).

For carotid imaging, a custom built 4-channel phased-array receiver coil was used to optimize the signal-to-noise ratio. Patients were positioned supine, without cardiac triggering and free breathing. Localization of the carotid was obtained with both fast gradient echo and time of flight sequences. Imaging covered the carotid bifurcation and approximately 3 cm above and below. Transverse images were acquired using Rapid Extended coverage (REX)[18, 19], double-inversion recovery (DIR) and turbo-spin echo (TSE) techniques. Proton density weighted (PDW) and T2-weighted (T2W) images were acquired with the following parameters: slice thickness = 3 mm; inter-gap slice = 0.3 mm; repetition time, 2130ms/2130ms (PDW/T2W images); echo time 5.6ms/56ms (PDW/T2W images); field of view (FOV) 12 cm; acquisition Matrix 256×256; no phase wrap; number of signal average 2/4 (PDW/T2W images); turbo factor (Echo train length): 15/15 (PDW/T2W images); receiver bandwidth: 488 Hz/pixel; no zero filling; 7 slices acquired simultaneously with 4 dark blood blocks, inversion time = 157 ms and chemical shift suppression pulse was added to suppress the signal from the perivascular fat.

Common femoral artery (CFA) and superficial femoral artery (SFA) imaging was performed using a six element spine array along with a 2-channel anterior body coil. Localizer images were obtained from the aortic bifurcation to the mid thigh. Images were acquired with turbo-spin echo (TSE) technique. PDW and T2W images were achieved with the following parameters: slice thickness = 3 mm, inter-gap slice = 1.5 mm; Repetition Time, 3500ms/ 3500ms (PDW/T2W Images); Echo Time 4.7ms/46ms (PDW/T2W Images); Field of view (FOV) 30 cm; acquisition matrix 384×382/ 320×284 (PDW/T2W Images); number of signal average 4/4 (PDW/T2W Images).

Data analysis

Image coregistration—Anatomical coregistration was done by viewing CT and T2W MR images simultaneously on the Advantage Workstation, 4.2 (General Electric, Milwaukee, Wisconsin). CT and MR images were carefully matched using anatomical landmarks. The carotid bifurcation was used for the neck imaging studies, whilst the inguinal ligament and the shape of the sartorius and adductor muscles guided coregistration of the femoral artery imaging studies. Two observers analyzed slice by slice all studies in every subject. Occasional slices had to be excluded because of poor image quality. Following PET/CT and MR image coregistration, one observer analyzed the MR dataset and another independently analyzed the corresponding PET/CT dataset.

Measurement of FDG uptake—The PET/CT images were transferred to a Xeleris workstation (General Electric, Milwaukee, Wisconsin). The carotid artery was divided anatomically into internal and common carotid arteries; similar distinction was made for the femoral studies (common and superficial). Arterial FDG uptake was measured by drawing circular regions of interest (ROI) on every slice of the co-registered PET/CT images. The ROI was fitted to the artery wall on each axial slice and other views (coronal and sagittal) were used to ensure that the FDG uptake was from the artery. The mean arterial standardized uptake value (SUV) was recorded on every axial slice along the vessel length. The mean artery SUV value was normalized to the blood pool SUV value measured from

the jugular vein or the inferior vena cava. The result was the mean arterial tissue-to-background ratio (TBR)[11], a reflection of true arterial FDG uptake.

Vessel quantitative analysis with MRI—Quantitative analysis of MR vessel wall images was performed with the 'Vessel Mass' software package (Leiden University Medical Center, The Netherlands). ROI capturing the inner and outer borders of the vessel wall were drawn onto every axial slice on T2W MR images. The following parameters were derived from the ROIs: mean vessel wall thickness (VWT), lumen area, vessel wall area (VWA) and total vessel area (TVA).

Plaque characterization with CT and MRI—The CT and MR images were transferred onto the Advantage Workstation (General Electric, Milwaukee, Wisconsin). After coregistration, every slice on CT had matching T2W and PDW slices. The CT data was used to detect the presence of calcification. If present, the plaque was classified as 'calcium' group. If not calcified, further plaque characterization by MR was based on the qualitative analysis of the signal intensity of the artery wall on T2W and PDW images using established criteria (Table 2.) [20, 21]. Collagen component was defined as iso- to hyperintense on T2W images and hyperintense on PDW images (Fig. 1a). Lipid-necrotic core was defined as hypo- or isointense on T2W images and hypo- or isointense on PDW images (Figs 1b and 2a). Using these criteria, plaques were characterized as being in the calcium group, the collagen group or the lipid core group.

Each plaque group was also subdivided according to the median value of the VWT: above the median value = subgroup A and below the median value = subgroup B.

Statistical analysis

To assess the relationships between mean TBR values across the three plaque groups, the non-parametric Mann-Whitney test was used. To assess the influence of the VWT on TBR in each group, the Mann-Whitney test was also used. The Spearman's rank correlation was used to study the relationships between mean TBR value and the following: VWT, VWA, and TVA. A value of $P < 0.05$ was considered significant.

Results

Nine patients underwent carotid imaging and seven had femoral artery imaging performed. After coregistration, 346 slices (collagen group = 253, lipid-necrotic core group = 41 and calcium group = 52) were included in the analysis.

Imaging parameters

The mean TBR value in each plaque group is given in Fig. 3. The lipid-necrotic core group had significantly higher mean TBR values than the collagen ($p < 0.001$) and calcium groups ($p < 0.001$). There was no difference in mean TBR levels between the collagen (1.19 (interquartile range (IQR) = 1.03–1.35) and calcium group (0.92 (IQR= 0.92–1.38) $p = 0.66$).

Fig. 4 illustrates the relationship between plaque morphology, composition and mean TBR. The plaques were divided into thin and thick walled subtypes based on the median vessel wall thickness of the subgroup. The lipid-necrotic core group had a median vessel wall thickness of 19 mm. There was a significant difference ($p=0.03$) in mean TBR in plaques with a mean vessel wall thickness lower than and those higher than 19 mm (mean TBR: 1.26 ± 0.25 vs. 1.50 ± 0.12). However, no such differences existed when the collagen and

calcium groups were sub-divided according to their mean vessel wall thickness (p = 0.37 and p = 0.68 respectively) (Fig. 4).

Except for the mean vessel wall thickness (r=0.041, p=0.447) the correlations between the mean TBR and the MRI parameters, including mean vessel wall thickness (r= 0.041, p=0.447), mean lumen area (r=0.402, p<0.00001), mean vessel wall area (r=0.29, r=0.402, p<0.00001), mean total vessel area (r=0.41, p<0.00001)) were significant, albeit weak.

Discussion

We prospectively compared the accumulation of FDG by PET-CT across different plaque morphology and compositions defined by MRI, in both carotid and femoral arteries. We chose to study carotid and femoral arteries together since the pathobiology of atherosclerosis is thought to be similar in both arterial beds[22].

We demonstrated higher vascular FDG uptake within lipid-rich plaques. The arteries with collagen and those containing calcium on MRI showed a similar and lower FDG uptake on PET-CT.

The difference in FDG uptake between the plaques maybe due to a smaller number of macrophages and their activity in the different types of plaques. This hypothesis is supported by the work of Tawakol et al. who showed, in a rabbit model of atherosclerosis a strong correlation between macrophage density and FDG uptake[24] and reported similar findings in patients with carotid artery disease[11].

Using complementary imaging methods allows a non-invasive characterization of both plaque composition and inflammatory activity. Our data suggest that those plaque types deemed high risk by the AHA criteria were in fact the one with the most FDG uptake. Collagen-rich and calcified plaques were low in their accumulation of FDG.

We also evaluated the mean tissue-to-background ratio (TBR) value according to a cutoff defined as the median of the mean vessel wall thickness in each group. The lipid-necrotic core group was the only one to display the following relationships: high TBR/thick vessel wall, low TBR/thin vessel wall. These findings are in keeping with pathologic studies that point to plaques with large lipid cores being at high risk of rupture[23].

Study limitations

Our study is limited by the small number of patients. Moreover, due to the limited spatial resolution of the PET/CT, around 5 mm, the partial volume effect is likely to influence the results. We did not examine the fibrous cap thickness in this study. This measure has also been shown to be a predictor of subsequent plaque rupture events[22, 25]. This could be achieved usingT1 weighted MRI sequences, or by using MRI contrast agents to highlight the cap. We are currently undertaking such studies in patients with carotid disease to investigate whether fibrous cap thickness has any bearing on plaque inflammation.

Conclusion

In this study, two high-risk aspects of atherosclerosis were determined by FDG-PET/CT and by MRI (T2W and PDW images). Atherosclerotic plaque inflammation is greater within lipid-rich plaques, and is proportional to the vessel wall thickness. After further, prospective validation studies, these non-invasive measurements could help to determine risk of clinical events within individual patients.

Acknowledgments

Acknowledgements and funding

This study is supported by the National Institutes of Health (grants R01 HL71021R01, R01 HL78667).

Work described in this paper was part-funded by the NIHR Cambridge Biomedical Research Centre.

Dr. Rudd is an International Fellowship holder from the British Heart Foundation.

References

1. Naghavi M, Libby P, Falk E, et al. From vulnerable plaque to vulnerable patient: a call for new definitions and risk assessment strategies: Part II. Circulation. 2003; 108:1772–1778. [PubMed: 14557340]
2. Naghavi M, Libby P, Falk E, et al. From vulnerable plaque to vulnerable patient: a call for new definitions and risk assessment strategies: Part I. Circulation. 2003; 108:1664–1672. [PubMed: 14530185]
3. Randomised trial of cholesterol lowering in 4444 patients with coronary heart disease: the Scandinavian Simvastatin Survival Study (4S). Lancet. 1994; 344:1383–1389. [PubMed: 7968073]
4. MRC/BHF Heart Protection Study of cholesterol lowering with simvastatin in 20,536 high-risk individuals: a randomised placebo-controlled trial. Lancet. 2002; 360:7–22. [PubMed: 12114036]
5. Crisby M, Nordin-Fredriksson G, Shah PK, Yano J, Zhu J, Nilsson J. Pravastatin treatment increases collagen content and decreases lipid content, inflammation, metalloproteinases, and cell death in human carotid plaques: implications for plaque stabilization. Circulation. 2001; 103:926–933. [PubMed: 11181465]
6. Davies MJ. Stability and instability: two faces of coronary atherosclerosis. The Paul Dudley White Lecture 1995. Circulation. 1996; 94:2013–2020. [PubMed: 8873680]
7. Kolodgie FD, Virmani R, Burke AP, et al. Pathologic assessment of the vulnerable human coronary plaque. Heart. 2004; 90:1385–1391. [PubMed: 15547008]
8. Schaar JA, Muller JE, Falk E, et al. Terminology for high-risk and vulnerable coronary artery plaques. Report of a meeting on the vulnerable plaque, June 17 and 18, 2003, Santorini, Greece. Eur Heart J. 2004; 25:1077–1082. [PubMed: 15191780]
9. Bengel FM. Vascular FDG uptake: further steps toward clinical acceptance. J Nucl Cardiol. 2008; 15:154–156. [PubMed: 18371583]
10. Rudd JH, Warburton EA, Fryer TD, et al. Imaging atherosclerotic plaque inflammation with [18F]-fluorodeoxyglucose positron emission tomography. Circulation. 2002; 105:2708–2711. [PubMed: 12057982]
11. Tawakol A, Migrino RQ, Bashian GG, et al. In vivo 18F-fluorodeoxyglucose positron emission tomography imaging provides a noninvasive measure of carotid plaque inflammation in patients. J Am Coll Cardiol. 2006; 48:1818–1824. [PubMed: 17084256]
12. Yuan C, Mitsumori LM, Ferguson MS, et al. In vivo accuracy of multispectral magnetic resonance imaging for identifying lipid-rich necrotic cores and intraplaque hemorrhage in advanced human carotid plaques. Circulation. 2001; 104:2051–2056. [PubMed: 11673345]
13. Cai JM, Hatsukami TS, Ferguson MS, Small R, Polissar NL, Yuan C. Classification of human carotid atherosclerotic lesions with in vivo multicontrast magnetic resonance imaging. Circulation. 2002; 106:1368–1373. [PubMed: 12221054]
14. Davies JR, Rudd JH, Fryer TD, et al. Identification of culprit lesions after transient ischemic attack by combined 18F fluorodeoxyglucose positron-emission tomography and high-resolution magnetic resonance imaging. Stroke. 2005; 36:2642–2647. [PubMed: 16282536]
15. Rudd JH, Myers KS, Bansilal S, et al. (18)Fluorodeoxyglucose positron emission tomography imaging of atherosclerotic plaque inflammation is highly reproducible: implications for atherosclerosis therapy trials. J Am Coll Cardiol. 2007; 50:892–896. [PubMed: 17719477]
16. Kinahan PE, Rogers JG. Analytic 3D image reconstruction using all detected events. IEEE Trans Nucl Sci. 1989; 36:964–968.

17. Gundlich B, Musmann P, Weber S, Nix O, Semmler W. From 2D PET to 3D PET: issues of data representation and image reconstruction. Z Med Phys. 2006; 16:31–46. [PubMed: 16696369]

18. Mani V, Itskovich VV, Aguiar SH, et al. Comparison of gated and non-gated fast multislice black-blood carotid imaging using rapid extended coverage and inflow/outflow saturation techniques. J Magn Reson Imaging. 2005; 22:628–633. [PubMed: 16215965]

19. Mani V, Itskovich VV, Szimtenings M, et al. Rapid extended coverage simultaneous multisection black-blood vessel wall MR imaging. Radiology. 2004; 232:281–288. [PubMed: 15220509]

20. Fuster V, Fayad ZA, Moreno PR, Poon M, Corti R, Badimon JJ. Atherothrombosis and high-risk plaque: Part II: approaches by noninvasive computed tomographic/magnetic resonance imaging. J Am Coll Cardiol. 2005; 46:1209–1218. [PubMed: 16198833]

21. Yuan C, Mitsumori LM, Beach KW, Maravilla KR. Carotid atherosclerotic plaque: noninvasive MR characterization and identification of vulnerable lesions. Radiology. 2001; 221:285–299. [PubMed: 11687667]

22. Virmani R, Ladich ER, Burke AP, Kolodgie FD. Histopathology of carotid atherosclerotic disease. Neurosurgery. 2006; 59:S219–S227. discussion S213-213. [PubMed: 17053606]

23. Mann JM, Davies MJ. Vulnerable plaque. Relation of characteristics to degree of stenosis in human coronary arteries. Circulation. 1996; 94:928–931. [PubMed: 8790027]

24. Tawakol A, Migrino RQ, Hoffmann U, et al. Noninvasive in vivo measurement of vascular inflammation with F-18 fluorodeoxyglucose positron emission tomography. J Nucl Cardiol. 2005; 12:294–301. [PubMed: 15944534]

25. Burke AP, Weber DK, Kolodgie FD, Farb A, Taylor AJ, Virmani R. Pathophysiology of calcium deposition in coronary arteries. Herz. 2001; 26:239–244. [PubMed: 11479935]

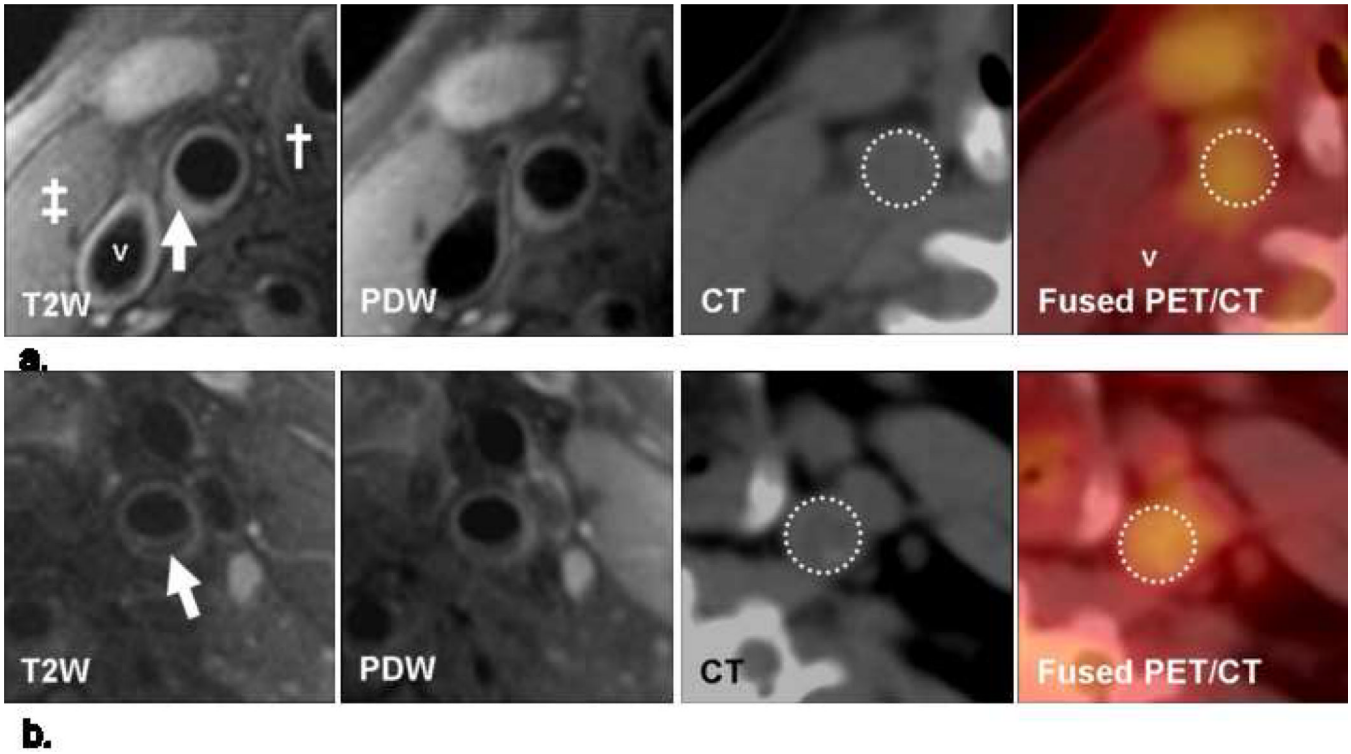

Fig 1.

(a) Transverse MR and FDG-PET/CT images demonstrating a collagen rich plaque of the right common carotid artery. The T2-weighted (T2W) image demonstrates the right common carotid artery (white arrow), the jugular vein ("v"), the sterno-cleido-mastoid muscle (‡) and the thyroid cartilage (†). Carotid artery wall appears hyperintense on T2W (white arrow) and on proton density weighted (PDW) images. CT confirms the absence of calcification in the artery wall. The right common carotid artery is displayed on the computed tomography (CT) and on the fused positron emission tomography/CT (PET/CT) images (white dashed circle).

(b) Transverse MR images and corresponding FDG-PET/CT images indicate a carotid artery lipid-necrotic core plaque, hypointense on T2W (white arrow) and on PDW images. CT image demonstrates the absence of calcification. The white dashed circle demonstrates FDG uptake into the entire artery section on the PET/CT image.

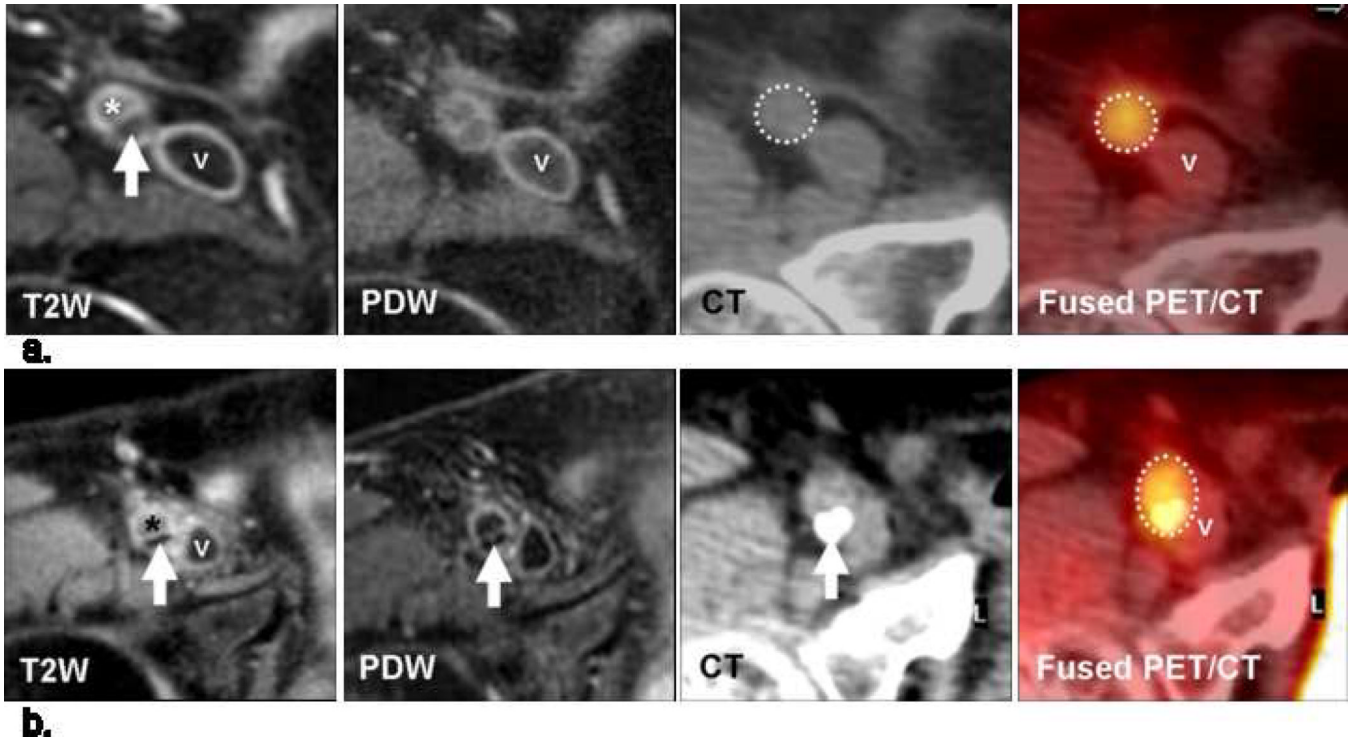

Fig 2.

Transverse MR and FDG-PET/CT images obtained at the same location in the right superficial femoral artery in two different patients.

(a) The lipid-necrotic core plaque is eccentric and hypointense on T2W (white arrow) and on proton density weighted (PDW) images. The absence of calcification in the vessel wall on CT in combination with the MR findings suggests a lipid rich plaque. FDG uptake is measured inside the white dashed circle display on the fused PET/CT image.

(b) Eccentric calcified plaque into the posterior wall of the superficial femoral artery, the lumen (*) is above and the superficial femoral vein (v) adjacent to the artery. The hypointense region on T2W (white arrow) and on PDW (white arrow) images is associated with a large hyperattenuated region on CT (white arrow).

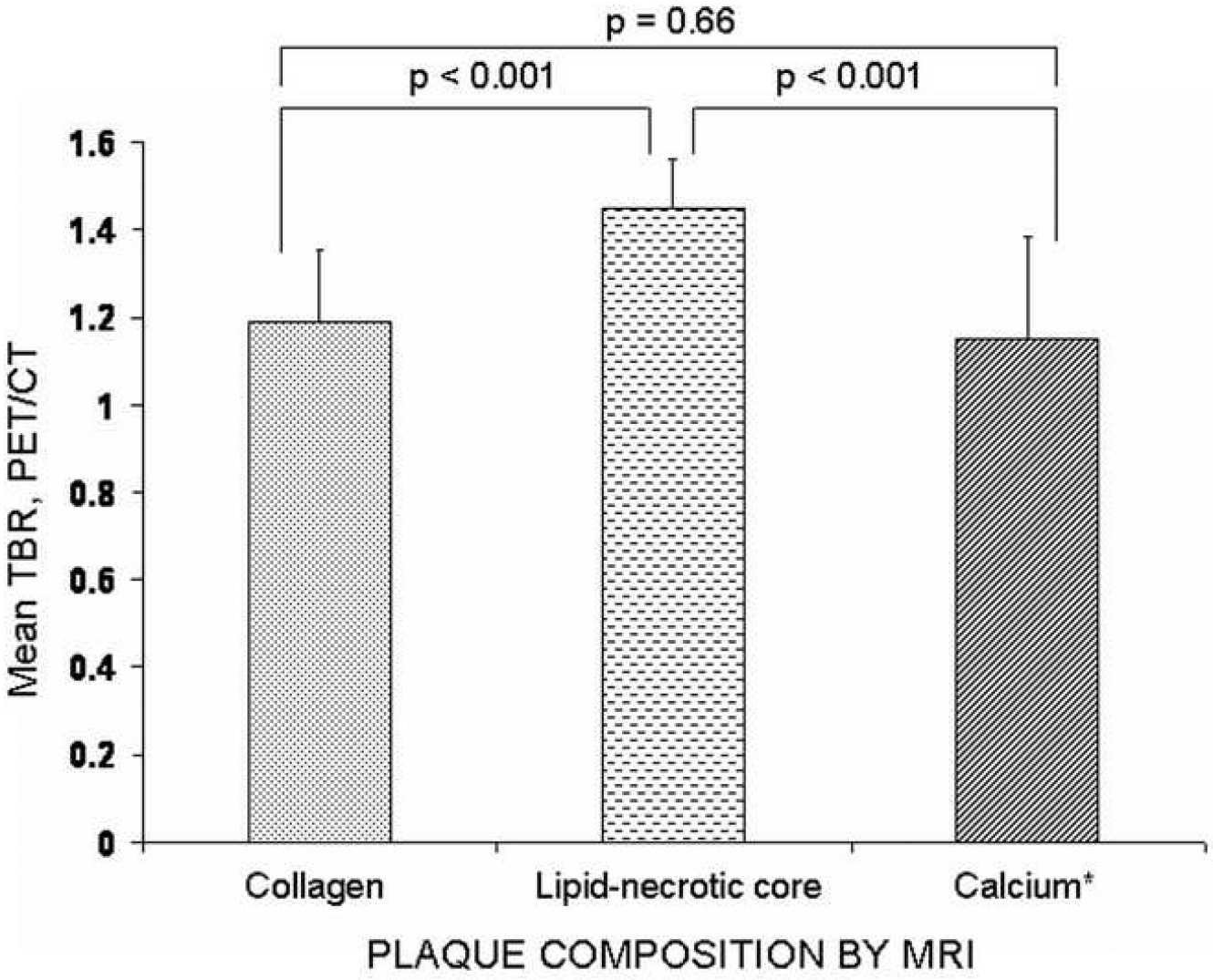

Fig 3.

Mean TBR values according to plaque composition.

Diagram depicts the relationship between mean tissue-to-background ratio (TBR) values and plaque composition. The lipid group had a higher mean TBR than the collagen ($p<0.001$) and calcium group ($p<0.001$). There was no difference in mean TBR levels between the collagen (1.19 (interquartile range (IQR) = 1.03 –1.35) and calcium group (0.92 (IQR= 0.92–1.38) $p = 0.66$).

Error bars indicate standard deviation and PET = positron emission tomography.

* Calcifications were defined by CT.

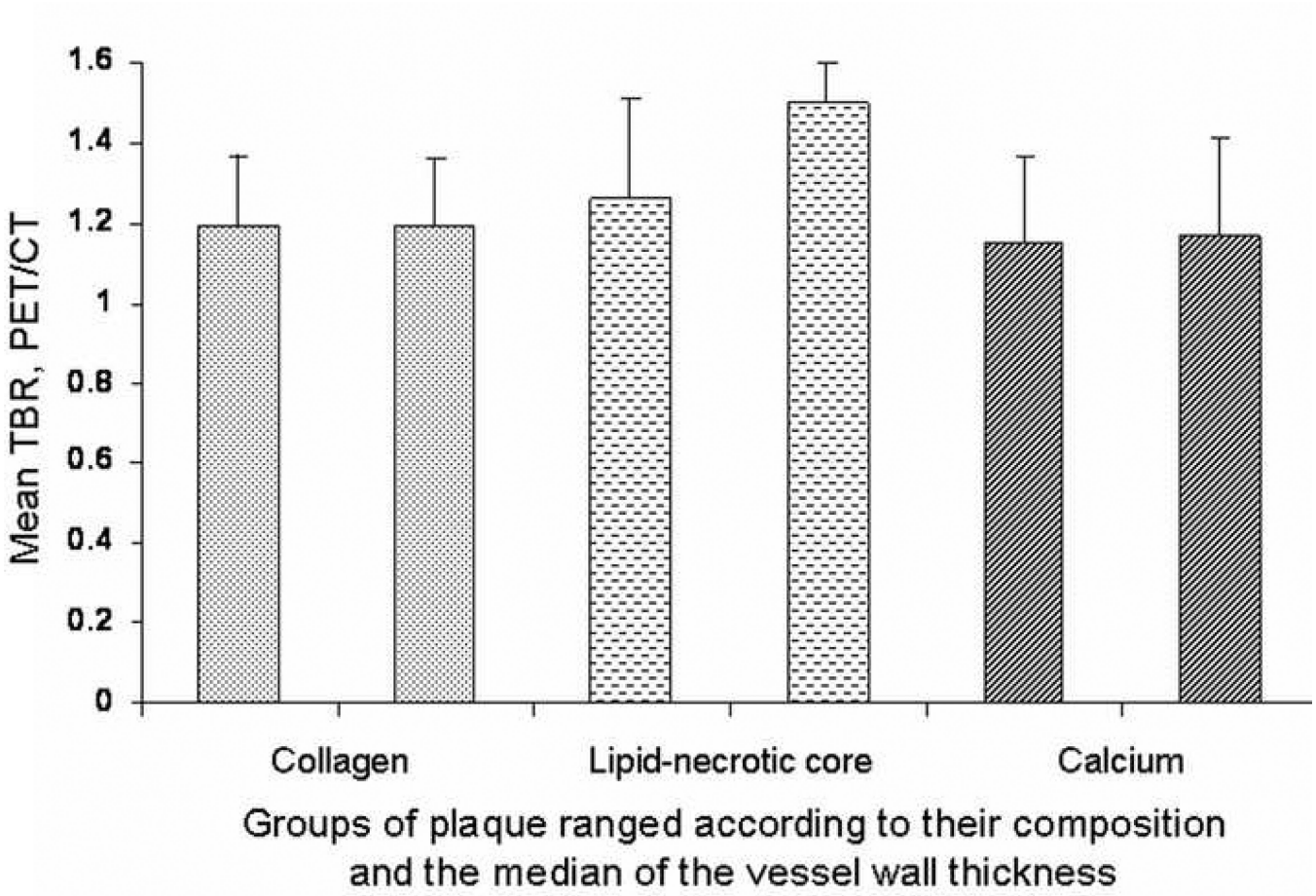

Fig 4.

Each group was divided according to the median of the vessel wall thickness (VWT): left below the cutoff and right above it. The threshold value is 16 mm for the collagen group, 19 mm for the lipid-necrotic core group and 16 mm for the calcium group.

VWT is correlated to the mean TBR values only if the plaque belongs to the lipid-necrotic core group. Mean TBR values and VWT are not correlated in the calcified or collagen plaque groups.

Error bars indicate standard derivation. TBR = tissue-to-background ratio; PET = positron emission tomography.

Table 1

Cardiovascular risk factors

Mean Body Mass Index (kg/m^2)	26 (SD±3.7)
Hypertension, n (%)	9 (56.25)
Diabetes, n (%)	4 (25)
Smoking, n (%)	2 (12.5)
History of CAD*, n (%)	11 (68.75)
History of stroke, n (%)	0 (0)
Statins use, n (%)	15 (93.75)

*CAD: Coronary Artery Disease

Table 2

MR Signal Intensity (SI) of Main Components of Atherosclerotic Plaque

Plaque component	T2W	PDW
Collagen	+/−to +	+
Lipid rich/ necrotic core	−to +/−	−to +/−

T2W indicates T2-weighted and PDW, proton density weighted.
SI relative to adjacent muscle.

+ Hyperintense.

+/− Isointense.

− Hypointense.